

1 **Tailoring barrier properties of thermoplastic corn starch-based films (TPCS) by**
2 **means of a multilayer design**

3
4 *María José Fabra^{1*}, Amparo López-Rubio¹, Luis Cabedo² and Jose M. Lagaron¹*

5
6 ¹Food Safety and Preservation Department, IATA-CSIC, Avda. Agustín Escardino 7,
7 46980 Paterna (Valencia), Spain, email: mjfabra@iata.csic.es

8 ²Grupo de Polímeros y Materiales Avanzados (PIMA), Universitat Jaume I, Castellón,
9 España

10

11

12

13

14

15

16

17

18

19

20

21

22

23

24

25

26 **Abstract**

27 This work compares the effect of adding different biopolyester electrospun coatings
28 made of polycaprolactone (PCL), polylactic acid (PLA) and polyhydroxybutyrate
29 (PHB) on oxygen and water vapour barrier properties of a thermoplastic corn starch
30 (TPCS) film. The morphology of the developed multilayer structures was also examined
31 by Scanning Electron Microscopy (SEM). Results showed a positive linear relationship
32 between the amount of the electrospun coatings deposited onto both sides of the TPCS
33 film and the thickness of the coating. Interestingly, the addition of electrospun
34 biopolyester coatings led to an exponential oxygen and water vapour permeability drop
35 as the amount of the electrospun coating increased. This study demonstrated the
36 versatility of the technology here proposed to tailor the barrier properties of food
37 packaging materials according to the final intended use.

38

39

40 **Keywords:** TPCS, Electrospinning, Multilayer, Barrier properties, Biopolyesters.

41

42 **1. INTRODUCTION**

43 The use of biopolymers has received increased attention in the last decades as potential
44 substitutes for conventional polymers in a broad range of applications. Among
45 biopolymers, polysaccharides, like starch, are interesting renewable resources that have
46 different applications. Indeed, the introduction of starch in the plastic sector has been
47 motivated by its low cost and biodegradability and by the fact that it is available in large
48 quantities (Xu *et al.*, 2005). However, starch cannot be processed through conventional
49 plastic equipment without further modification because its degradation begins at a
50 temperature lower than its melting point (Avérous, 2004). By the addition of water or
51 other plasticizers such as glycerol or sorbitol, the native crystalline structure of starch is
52 irreversibly disrupted (the so-called gelatinization phenomenon) and thus, the granular
53 starch is transformed into a thermoplastic starch (TPS) which vary from a soft material
54 (high plasticizer level) to a brittle material (low plasticizer level) depending on the
55 moisture and plasticizer level (Jiménez *et al.*, 2012).

56 The barrier to water vapor and oxygen are two essential properties to consider in starch-
57 based materials because oxygen and water molecules can deteriorate food properties.
58 Indeed, one of the main problems of starch-based films is their high water sensitivity
59 arising from their hydrophilic character, which leads to strong plasticization (Yan *et al.*,
60 2012). This effect negatively affects some characteristics such as the oxygen barrier
61 properties, which are excellent at low hydration levels and plasticizer content but
62 decrease as water sorption increases (Jiménez *et al.*, 2013, Yan *et al.*, 2012). Therefore,
63 many research works have focused on improving starch performance either by blending
64 it with other moisture resistant biodegradable polymers such as polylactic acid (PLA)
65 and polycaprolactone (PCL) (Ali Akbari Ghavimi *et al.*, 2015, Ayana *et al.*, 2014, Cai *et*
66 *al.*, 2014, Matzinos *et al.*, 2002, Ortega-Toro *et al.*, 2015) or through the addition of

67 dispersed nanoreinforcing agents to generate nanobiocomposites (Dean *et al.*, 2008,
68 Zeppa *et al.*, 2009). However, from an industrial implementation point of view, it is
69 important to highlight that complex multilayer structures are suggested as an alternative
70 to improve the performance of biopolymers, being the most efficient form to constitute
71 barrier materials (Fabra *et al.*, 2013, 2014). Whilst this multilayer design has been
72 widely used for synthetic materials, it has been scarcely developed for biodegradable
73 food packaging systems due to technological problems associated to the scaling-up
74 process and multilayer assembly. Nowadays, this methodology is being successfully
75 exploited by means of electrohydrodynamic processing, also known as electrospinning,
76 to improve the barrier and functional performance of biodegradable polymers
77 thermodynamically immiscible with the additional advantages of forming electrospun
78 coatings (Fabra *et al.*, 2014) or bioadhesives (Fabra *et al.*, 2015 ab) which show
79 excellent adhesion between layers, avoiding the use of synthetic adhesives.
80 Taking advantage of the methodology already described, this paper reports, for the first
81 time, a comparative study in which the effect of different amounts of electrospun
82 biopolyesters coatings (polylactic acid –PLA-, polycaprolactone –PCL- and
83 polyhydroxybutyrate –PHB-) has been analyzed and compared in terms of barrier
84 efficiency.

85

86 **2. MATERIALS AND METHODS**

87 **2.1 Materials**

88 Polyhydroxybutyrate (PHB) pellets were supplied by Biomer (Krailling, Germany).
89 PHB was reported to have 0-40 wt% of plasticizers and an unreported amount of non-
90 toxic nucleating agents to improve melt processing (Hänggi, 2011). The semicrystalline
91 polylactide (PLA) used was a film extrusion grade produced by Natureworks (with a D-

92 isomer content of approximately 2%). The molecular weight had a number-average
93 molecular weight (M_n) of ca. 130,000 g/mol, and the weight average molecular weight
94 (M_w) was ca. 150,000 g/mol as reported by the manufacturer. The polycaprolactone
95 (PCL) grade FB100 was supplied by Solvay Chemicals (Belgium).
96 Corn starch (CS) was kindly supplied by Roquette (Roquette Laisa España, Benifaio,
97 Spain) and glycerol (Panreac Quimica, S.A. Castellar Del Vallés, Barcelona, Spain) was
98 used as plasticizer.
99 N,N-dimethylformamide (DMF) with 99% purity and trichloromethane (99% purity)
100 were purchased from Panreac Quimica S.A. (Barcelona, Spain). 2,2,2-Trifluoroethanol
101 (TFE) with 99% purity were purchased from Sigma-Aldrich (Spain). All products were
102 used as received without further purification.

103

104 **2.2. Preparation of films**

105 2.2.1 Preparation of thermoplastic corn starch films (TPCS)

106 Corn starch and glycerol, as plasticizer, were dispersed in water using a polymer:
107 glycerol: water ratio of 1:0.3:0.5 (w/w/w) and the dispersion was melt-mixed in a
108 Brabender Plastograph internal mixer at 130°C and 60 rpm for 4 minutes. The mixture
109 was then spread evenly on Teflon and placed in a compression mould (Carver 4122,
110 USA) at a pressure of 30000 lbs and 130°C for 5 minutes.

111

112 2.2.2 Preparation of multilayers TPCS systems

113 TPCS films were coated with PHB, PLA or PCL mats produced by means of the
114 electrospinning technique. PHB solutions in 2,2,2-trifluoroethanol having a total solids
115 content of 10 wt.% were used to generate the electrospun fibres. The PLA and PCL
116 electrospinning solutions were prepared by dissolving the required amount of the

117 biopolymer, under magnetic stirring, in a solvent prepared with a mixture of
118 trichloromethane (TCM):N,N-dimethylformamide (DMF) in order to reach a 5 or 12 %
119 in weight (wt.-%) of PLA and PCL, respectively. The TCM:DMF ratio used for PLA
120 and PCL was 85:15 and 65:35, respectively.

121 PHB, PLA or PCL fibre mats were directly electrospun onto both sides of the TPCS
122 films by means of a Fluidnatek® electrospinning pilot plant equipment from Bioinicia
123 S.L. (Valencia, Spain) equipped with a variable high-voltage 0-60 kV power supply.
124 Biopolyester solutions were electrospun under a steady flow-rate using a motorized high
125 throughput multinozzle injector, scanning vertically towards a metallic grid used as
126 collector, in which the neat TPCS film was attached. The distance between the needle
127 and the collector was 20, 24 and 31 cm for PHB, PLA and PCL, respectively, and the
128 experiments were carried out at ambient temperature. The voltage of the collector and
129 injector were set at 24 kV and 19 kV, respectively.

130 Different deposition times (0, 2, 10, 20, 40, 60 and 90 minutes), were evaluated in the
131 TPCS film to see how deposition time affected barrier properties. The total amount of
132 electrospun material (mg cm^{-1}) was estimated by weighing the TPCS film before and
133 after collection of the electrospun material.

134 With the aim of obtaining transparent and continuous outer layers based on PHB, PLA
135 or PCL, an additional heating step was applied. Coated TPCS films were placed
136 between hot plates at 160°C to melt and homogenize the PHB or PLA phase and 60°C to
137 melt the PCL layer.

138

139 **2.3. Characterization of films**

140

141 2.3.1. Scanning Electron Microscopy (SEM)

142 A Hitachi S-4800 microscope (Hitachi High Technology Corp., Tokyo, Japan) was used
143 to observe the morphology of films cross-sections. Cross-sections of the samples were
144 prepared by cryo-fracture of the films using liquid N₂. The samples were mounted on
145 bevel sample holders with double-sided adhesive tape, and sputtered with Au/Pd under
146 vacuum. Samples were observed using an accelerating voltage of 10 kV and a working
147 distance of 12–16 mm. Layer thicknesses were measured by means of the Adobe
148 Photoshop CS3 extended software from the SEM micrographs in their original
149 magnification.

150

151 2.3.3. Barrier properties

152

153 *2.3.3.1 Water Vapour Permeability (WVP)*

154 The WVP of TPCS and multilayer structures was determined by using the ASTM
155 (2011) gravimetric method using Payne permeability cups (Elcometer SPRL,
156 Hermelle/s Argenteau, Belgium) of 3.5 cm diameter. For each type of samples,
157 measurements were done in triplicate and water vapour permeability was carried out at
158 25°C and 0-100% relative humidity gradient, which was generated by using dry silica
159 gel and distilled water, respectively. The cups were weighed periodically (0.0001 g)
160 after the steady state was reached. Cups with aluminium films were used as control
161 samples to estimate solvent loss through the sealing. Water vapour transmission rate
162 (WVTR) was calculated from the steady-state permeation slopes (8 points) obtained
163 from the regression analysis of weight loss data vs. time (Eq. 1), and weight loss was
164 calculated as the total cell loss minus the loss through the sealing.

165

$$166 \quad WVTR = \Delta m / (\Delta t \cdot A) \quad (Eq. 1)$$

167 where $\Delta m/\Delta t$, is the weight of moisture loss per unit of time (Kg/s); A, the film area
168 exposed to moisture transfer (m^2).

169 Water vapour permeance was calculated using equation 2 as a function of p_1 (water
170 vapor pressure on the film's inner surface) and p_2 (pressure on the film's outer surface in
171 the cabinet).

$$172 \text{ Permeance} = \text{WVTR} / (p_1 - p_2) \text{ (Eq. 2)}$$

173 Water vapour permeability (WVP) was obtained by multiplying the permeance by the
174 average film thickness as specified in equation 3:

$$175 \text{ WVP} = \text{permeance} \cdot \text{thickness} \text{ (Eq. 3)}$$

176 Films thickness was measured in at least 5 different points using a digital micrometer
177 (Mitutoyo, Spain) with ± 0.001 mm accuracy.

178

179 *2.3.3.2 Oxygen permeability (O_2P)*

180 The O_2P was derived from oxygen transmission rate (OTR) measurements recorded, in
181 triplicate, using an Oxygen Permeation Analyzer M8001 (Systech Illinois, UK) at 80%
182 RH and 23°C. A sample of each multilayer film (5 cm^2) was placed in the test cell and
183 pneumatically clamped in place. The samples were previously purged with nitrogen in
184 the humidity equilibrated samples, before exposure to an oxygen flow of 10 mL min^{-1} .
185 In order to obtain the oxygen permeability (OP) (Eq. 4), film thickness was considered
186 in each case.

$$187 \text{ OP} = \text{permeance} \cdot \text{thickness} \text{ (Eq. 4)}$$

188

189

190 *2.3.4. Contact Angle Measurements*

191 Measurements of contact angle were performed at room conditions (*ca.* 23°C and 53%
192 RH) in a Video-Based Contact Angle Meter model OCA 20 (Data Physics Instruments
193 GmbH, Filderstadt, Germany). Data were obtained by analysing the shape of a distilled
194 water drop after it had been placed over the film for 5 s. Image analyses were carried
195 out by SCA20 software. At least, eight replicates were made for each sample.

196

197 **2.4. Statistical Analysis**

198 Statistical analysis was performed using the analysis of variance procedure (ANOVA)
199 with StatGraphics Plus version 5.1 (Statistical Graphics Corp.). Fisher's Least
200 Significant Difference (LSD) test was applied to detect differences of means, and
201 $p < 0.05$ (95% significant level) was considered to be statistically significant.

202

203 **3. RESULTS AND DISCUSSION**

204 **3.2 Microstructure of multilayer films**

205 Since it is well-known that barrier properties of biopolymers are strongly related to their
206 morphology, SEM was used to evaluate the films' homogeneity, layer structure,
207 presence of pores and cracks, surface smoothness and thickness. SEM micrographs of
208 the surface images of the multilayer TPCS-based films are shown in Figure 1. TPCS
209 film presented homogeneous and smooth surfaces, without visible pores and cracks (see
210 Figure 1). Besides, it was clearly observed that annealing the PCL, PLA and PHB fibres
211 favoured the formation of a continuous coating layer which could contribute to improve
212 the barrier properties of the TPCS films.

213 The cross-section image of the TPCS film showed a compacted structure with absence
214 of intact starch granules, demonstrating the effectiveness of the destructure and
215 thermo-compression processes (*cf.* Figure 2A). Representative images of the multilayer

216 structures prepared with PCL, PLA or PHB are shown in Figures 2, 3 and 4,
217 respectively. The first clear observation of these multilayer films was that all samples
218 exhibited a laminate-like structure in which relatively homogeneous biopolyester
219 coatings were formed onto both sides of the TPCS films. Furthermore, the adhesion
220 between the outer layers and the TPCS film was very good and only a weak
221 delamination occurred after cryo-fracturing the material in some of the samples.

222 From the cross-section micrographs, it is also interesting to note that the thickness of the
223 outer layer depended on the biopolyester used and thus, on the electrospinning solutions
224 and the morphology of the electrospun fibres. Therefore, the amount of the coating layer
225 was estimated by weighting the TPCS before and after the electrospinning process and
226 it was observed that, for a given amount of the electrospun layer, the thickness of the
227 coating was governed by the polymer concentration used in the electrospinning solution
228 and the diameter of the electrospun fibres (Pérez-Masiá *et al.*, 2013; Chalco-Sandoval *et*
229 *al.*, 2014). A lineal relationship was observed between the thickness and the deposited
230 amount of the electrospun coating, as it will be detailed below (see Figure 5). In this
231 sense, for a given amount of the electrospun layer (*i.e.* 5 mg·cm⁻²), PHB provided
232 thicker layers and PLA the thinnest ones. As it was previously reported by Pérez-Masiá
233 *et al.*, 2013, PLA fibres were thinner than those obtained for PCL and PHB, in identical
234 electrospinning conditions as the ones applied in the present work. Therefore, after the
235 annealing process, PLA fibres were better compacted than PCL and PHB thus providing
236 thinner layers. Besides, when comparing the thicker ones (PCL and PHB), an excellent
237 interfacial adhesion between PCL and thermoplastic starch (TPS) melt phases have been
238 reported elsewhere (Ortega-Toro *et al.*, 2015, Cai *et al.*, 2014) in composite PCL/TPS
239 films which could also contribute to the increased attractive forces through hydrogen
240 bonding interactions between the ester carbonyl of PCL and the –OH groups of starch,

241 thus, reducing the thickness of the outer PCL layers when compared to the PHB layer
242 thickness. This interaction could lead to lowering the interfacial tension between both
243 materials, leading to compatibilization (Cai *et al.*, 2014). This could also explain the
244 good adhesion between PCL and TPCS layers.

245

246 **3.3 Barrier properties**

247 Figures 5 and 6 show the water vapour (WVP) and oxygen permeability (O₂P) values of
248 the neat TPCS films and the developed multilayer structures. Water and oxygen barrier
249 properties of the uncoated TPCS films developed in this work were in the same order as
250 those reported in the literature for films prepared by melt-compounding (Ortega-Toro *et*
251 *al.*, 2015). However, comparing with the literature data, these films were less permeable
252 than their counterparts prepared by solvent casting (Jiménez *et al.*, 2012; Müller *et al.*,
253 2011, Pushpadas *et al.*, 2008). Thus, one can firstly conclude that the processing method
254 used during film-formation played an important role in the final properties of the films.
255 This can be ascribed to the fact that the casting process involved long drying times
256 which contributed to the formation of a more open microstructure due to the solvent
257 evaporation phenomenon, creating channels throughout which water molecules could
258 easily diffuse. However, using the compression-moulding method, polymer chains were
259 more compacted giving rise to a denser structure. A similar trend was observed
260 comparing other biopolymer matrices such as PHA (Fabra *et al.*, 2013) or PLA (Byun,
261 Kim and Whiteside, 2010; Rhim, Hong, and Ha, 2009; Sánchez-García and Lagaron,
262 2010ab).

263 Figure 5 displays the water vapour permeability values of the developed multilayer
264 structures. As mentioned on above, the thickness of the outer layers linearly increased
265 as the mg (PCL, PLA or PHB) ·cm⁻² increased, whatever the biopolyester used.

266 Interestingly, the WVP values decreased exponentially as the mg coating layer·cm⁻²
267 increased ($y=b\cdot e^{ax}$) and thus, it was shown that the addition of biopolyester coatings
268 significantly reduced the WVP of the neat TPCS film. The exponential equation
269 represents the WVP behaviour whose initial value is b and whose rate of decay at any
270 time equals a mg coating layer·cm⁻² its value at that time. It is well-defined that if $0 < e^{ax}$
271 < 1 , the function decays as x ($x = \text{mg} \cdot \text{cm}^{-2}$) increases and thus, thus, greater values of a
272 lead to faster rates of decay. PHB was more efficient in reducing water vapour
273 permeability of TPCS films than PCL and PLA biopolymers. This agrees with the
274 greater water vapour permeability values of the neat PLA and PCL films (1.2 and 1.4 kg
275 Pa⁻¹ m⁻² s⁻¹, for PLA and PCL respectively) (Ambrosio-Martin *et al.*, 2014; Bychuk,
276 Kil'deeva and Cherdyntseva, 2014) as compared to the WVP obtained for a neat PHB
277 film (0.16 kg Pa⁻¹ m⁻² s⁻¹) (Plackett and Siró, 2011). Coefficients a , b and R^2 are given in
278 Table 1. The greater barrier efficiency on TPCS films is reflected through the lower a
279 and b and greater a values. Due to the abrupt permeability decrease for the multilayer
280 structures prepared with PHB as compared to the neat TPCS film, the regression
281 coefficient from the exponential model considering the whole mg PHB·cm⁻² range was
282 only ~0.93, so another fit only considering data of multilayer samples (without taking
283 into account the permeability of the neat TPCS film) was carried out, which allowed us
284 to make better predictions. The obtained values indicate that it is possible to use smaller
285 amounts of PHB electrospun outer layer than PLA or PCL to achieve the same barrier
286 efficiency. Concretely, for a given amount of electrospun coating (i.e. 5 mg ·cm⁻²), the
287 WVP of TPCS films dropped down to *ca.* 83, 88 and 91% for PCL, PLA and PHB
288 multilayer structures, respectively. Accordingly, the greatest reduction was observed
289 when coating the TPCS film with the greatest amount (expressed as mg·cm⁻²) of
290 electrospun PHB fibres, where the WVP dropped down to *ca.* 99 %.

291 A similar trend was observed for oxygen barrier properties, measured at 80% RH (*cf.*
292 Figure 6). The addition of electrospun coatings significantly reduced the oxygen
293 permeability and, the total amount of electrospun coating was also exponentially related
294 with oxygen barrier properties, being the PHB the biopolyester which provided the
295 greatest reduction in O_2P values. The coefficients a , b and R^2 of the fitting model are
296 given in Table 2. Once again, the greater barrier efficiency on TPCS films was
297 evidenced by the lower b values found for the multilayer structures prepared with PHB.
298 In fact, for a given amount of electrospun coating (*i.e.* $5 \text{ mg}\cdot\text{cm}^{-2}$), the oxygen
299 permeability of multilayer structures was improved up to $\sim 91\%$ for PLA and PCL and
300 $\sim 95\%$ for PHB as compared to the neat TPCS film. For oxygen barrier, the exponential
301 model was also reported considering only the data of PLA and PHB multilayer
302 structures (without the neat TPCS film), which allowed to make better predictions.
303 Thus, barrier results highlighted the suitability of this methodology to develop fully
304 biodegradable multilayer structures with improved barrier performance which could be
305 adapted depending on the final intended used.

306

307 **3.4 Contact angle**

308 The wettability properties of the TPCS films and the coated multilayer structures were
309 determined by direct measurement of contact angles of a water drop deposited on the
310 upper surface of the samples in order to investigate the effect of the PCL, PLA and PHB
311 coating layers on the surface water affinity. Contact angle was measured for the neat
312 TPCS and for multilayer structures prepared with the lowest and highest deposition
313 times. Since the deposition time did not match with the amount of biopolyester
314 deposited onto each side of the TPCS film, contact angle of multilayer structures
315 prepared with $3.2 \text{ mg}\cdot\text{cm}^{-2}$ electrospun coatings were also measured for comparative

316 purposes. The results are displayed in Table 3 and Figure 7, showing that all of them
317 (PCL, PLA and PHB) were quite effective (significantly greater contact angle values) in
318 protecting the TPCS inner layer from moisture. It might be noted that the resulted
319 contact angle values of the developed multilayer structures were in the same range as
320 for the neat PLA and PCL biopolymers (de Campos *et al.*, 2013; Chan *et al.*, 2013;
321 Darie *et al.*, 2014) although lower to contact angles reported in the literature for neat
322 PHB films (Zhijiang *et al.*, 2016). This difference could be ascribed to the intrinsic
323 plasticizer content in the original PHB pellets. As mentioned before, PHB was
324 originally reported to have between 0 and 40 wt% plasticizer in order to improve melt
325 processing (Hänggi, 2011).

326

327 **4. CONCLUSIONS**

328 Multilayer technology is a common and efficient technique used to improve the
329 physicochemical properties, mainly barrier, of the hydrophilic materials. In this work,
330 TPCS multilayer systems containing electrospun biopolyester outer layers based on PCL,
331 PLA or PHB have been developed. The incorporation of electrospun biopolyester
332 coating layers effectively improved water vapour and oxygen barrier properties of the
333 TPCS films, although the PHB was the most efficient in reducing both water and
334 oxygen permeability values.

335

336 **Acknowledgments**

337 The authors acknowledge financial support from MINECO (AGL2015-63855-C2-1).
338 M. J. Fabra is recipient of a Ramon y Cajal contract (RYC-2014-158) from the Spanish
339 Ministry of Economy and Competitiveness, respectively.

340

341 **REFERENCES**

- 342 Ali Akbari Ghavimi, S., Ebrahimzadeh, M.H., Solati-Hashjin, M., Abu Osman, N.A.
343 (2015). Polycaprolactone/starch composite: Fabrication, structure, properties, and
344 applications. *Journal of Biomedical Materials Research - Part A*, 103 (7), 2482-2498.
345 DOI: 10.1002/jbm.a.35371
- 346 Ambrosio-Martín, J., Fabra, M.J., Lopez-Rubio, A., and Lagaron, J.M. (2014). An
347 effect of lactic acid oligomers on the barrier properties of polylactide. *Journal of*
348 *Material Science*, 49(8), 2975-2986. DOI: 10.1007/s10853-013-7929-x
- 349 ASTM, 1995. Standard test methods for water vapour transmission of materials.
350 Standards designations: E96–95. In: Annual Book of ASTM Standards. *American*
351 *Society for Testing and Materials*, Philadelphia, PA, pp. 406–413.
- 352 Averous L. (2004). Biodegradable multiphase systems based on plasticized starch: A
353 review. *Journal of Macromolecular Science-Polymer Reviews*, 3, 231–274.
354 DOI:10.1081/MC-200029326
- 355 Ayana, B., Suin, S., Khatua, B.B. (2014). Highly exfoliated eco-friendly thermoplastic
356 starch (TPS)/poly (lactic acid)(PLA)/clay nanocomposites using unmodified nanoclay.
357 *Carbohydrate Polymers*, 110, 430-439. DOI: 10.1016/j.carbpol.2014.04.024
- 358 Bychuk, M.A., Kil'deeva, N.R., Cherdyntseva, T.A. (2014). Films of a biodegradable
359 polyester mixture with antimicrobial and proteolytic activity. *Pharmaceutical Chemistry*
360 *Journal*, 48 (1), 60-64. DOI: 10.1007/s11094-014-1047-1
- 361 Byun, Y., Kim, Y. T., and Whiteside, S. (2010). Characterization of an antioxidant
362 polylactic acid (PLA) film prepared with α -tocopherol, BHT and polyethylene glycol
363 using film cast extruder. *Journal of Food Engineering*, 100, 239-244. DOI:
364 10.1016/j.jfoodeng.2010.04.005

365 Cai, J., Xiong, Z., Zhou, M., Tan, J., Zeng, F., Ma, M., Lin, S. and Xiong, H. (2014).
366 Thermal properties and crystallization behavior of thermoplastic starch/poly(ϵ -
367 caprolactone) composites. *Carbohydrate Polymers*, 102, 746-754. DOI:
368 10.1016/j.carbpol.2013.10.095

369 Chan, R.T.H, Marçal, H., Ahmed, T., Russel, R.A., Holden, P.J., and Foster, L.J.R.
370 (2013). Poly(ethylene glycol)-modulated cellular biocompatibility of
371 polyhydroxyalkanoate films. *Polymer International*, 62, 884-892. DOI: 10.1002/pi.4451

372 Chalco-Sandoval, W., Fabra, M.J., Lopez-Rubio, A., Lagaron, J.M. (2014). Electrospun
373 heat management polymeric materials of interest in food refrigeration and packaging.
374 *Journal of Applied Polymer Science*, 131 (1) 40661. DOI: 10.1002/app.40661

375 Darie, R.M., Pâslaru, E., Sdrobis, A., Pricope, G.M., Hitruc, G.E., Poiata, A.,
376 Baklavaridis, A. and Vasile, C. (2014). Effect of Nanoclay Hydrophilicity on the
377 Poly(lactic acid)/Clay Nanocomposites Properties. *Industrial and Engineering*
378 *Chemistry Research*, 7877-7890. DOI: 10.1021/ie500577m

379 Dean, K.M., Do, M. D., Petinakis, E. and Yu, L. (2008): Key interactions in
380 biodegradable thermoplastic starch/poly(vinyl alcohol)/montmorillonite micro- and
381 nanocomposites. *Composite Science and Technology*, 68, 1453-1462.
382 DOI:10.1016/j.compscitech.2007.10.037

383 de Campos, A., Tonoli, G.H.D., Marconcini, J.M., MAttoso, L.H.C., Klamczynski, A.,
384 Gregorski, K.S., Wood, D., Williams, T., Chiou, B.-S., Imam, S.H. (2013). TPS/PCL
385 Composite Reinforced with Treated Sisal Fibers: Property, Biodegradation and Water-
386 Absorption. *Journal of Polymers and the Environment*, 21, 1-7. DOI: 10.1007/s10924-
387 012-0512-8

388 Fabra, M.J., López-Rubio, A., and Lagaron, J.M. (2013). High barrier
389 polyhydroxyalcanoate food packaging film by means of nanostructured electrospun

390 interlayers of zein. *Food Hydrocolloids*, 32, 106-114.
391 DOI:10.1016/j.foodhyd.2012.12.007

392 Fabra, M.J., López-Rubio, A. and Lagaron, J.M. (2014). Nanostructured interlayers of
393 zein to improve the barrier properties of high barrier polyhydroxyalkanoates and other
394 polyesters. *Journal of Food Engineering*, 127, 1-9.
395 DOI:10.1016/j.jfoodeng.2013.11.022

396 Fabra, M.J., López-Rubio, A. and Lagaron, J.M. (2015a). Effect of the film-processing
397 conditions, relative humidity and aging on wheat gluten films coated with electrospun
398 polyhydroxyalkanoate. *Food Hydrocolloids*, 44, 292-299.
399 DOI:10.1016/j.foodhyd.2014.09.032

400 Fabra, M.J., López-Rubio, A. and Lagaron, J.M. (2015b). Three-Layer Films Based on
401 Wheat Gluten and Electrospun PHA. *Food and Bioprocess Technology*, 8(11), 2330-
402 2340. DOI 10.1007/s11947-015-1590-0

403 Hänggi, U. J. (2011). Biomer biopolyesters. Germany: Krailling.

404 Hutchings, J. B. (1999). Food and colour appearance (2nd ed.). Gaithersburg,
405 M.D.:Chapman and Hall Food Science Book, Aspen Publication.

406 Jiménez, A., Fabra, M.J., Talens, P. and Chiralt, A. (2012). Edible and Biodegradable
407 Starch Films: A Review. *Food and Bioprocess Technology*, 5(6), 2058-2076. DOI:
408 10.1007/s11947-012-0835-4

409 Jiménez, A., Fabra, M.J., Talens, P. and Chiralt, A. (2013). Phase transitions in starch
410 based films containing fatty acids. Effect on water sorption and mechanical behaviour.
411 *Food Hydrocolloids*, 30 (1), 408-418. DOI:10.1016/j.foodhyd.2012.07.007

412 Matzinos P, Tserki V, Kontoyiannis A, Panayiotou C. (2002). Processing and
413 characterization of starch/polycaprolactone products. *Polymer Degradation and*
414 *Stability*, 1, 17–24. DOI: 10.1016/S0141-3910(02)00072-1

415 Müller, C. M. O., Laurindo, J. B., and Yamashita. (2011). Effect of nanoclay
416 incorporation method on mechanical and water vapor barrier properties of starch-based
417 films. *Industrial Crops and Products*, 33, 605–610. DOI:10.1016/j.indcrop.2010.12.021

418 Ortega-Toro, R., Contreras, J., Talens, P., Chiralt., A. (2015). Physical and structural
419 properties and thermal behaviour of starch-poly(eopen-caprolactone) blend films for
420 food packaging . *Food Packaging and Shelf Life*, 5, 10-20. DOI:
421 10.1016/j.fpsl.2015.04.001

422 Pérez-Masiá, R., López-Rubio, A., Fabra, M.J., and Lagaron, J.M. (2013).
423 Biodegradable Polyester-Based Heat Management Materials of Interest in Refrigeration
424 and Smart Packaging Coatings. *Journal of Applied Polymer Science*, 30(5), 3251-3262.
425 DOI: 10.1002/app.39555

426 Plackett, D., and Siro, I. (2011). Polyhydroxyalkanoates (PHAs) for food packaging. In
427 J. M. Lagaron (Ed.), *Multifunctional and nanoreinforced polymers for food packaging*.
428 Cambridge. UK: Woodhead Publishing Limited.

429 Pushpadass, H. A., Marx, D. B., and Hanna, M. A. (2008). Effects of extrusion
430 temperature and plasticizers on the physical and functional properties of starch films.
431 *Starch/Stärke*, 60, 527–538. DOI: 10.1002/star.200800713

432 Rhim, J. W., Hong, S. I., and Ha, C. S. (2009). Tensile, water vapor barrier and
433 antimicrobial properties of PLA/nanoclay composite films. *LWT - Food Science and*
434 *Technology*, 42, 612-617. DOI:10.1016/j.lwt.2008.02.015

435 Sánchez-García, M. D., and Lagaron, J. M. (2010a). On the use of plant cellulose
436 nanowhiskers to enhance the barrier properties of polylactic acid. *Cellulose*, 17, 987-
437 1004. DOI: 10.1007/s10570-010-9430-x

438 Sánchez-García, M. D., and Lagaron, J. M. (2010b). Novel Clay-Based
439 Nanobiocomposites of Biopolyesters with Synergistic Barrier to UV Light, Gas, and
440 Vapour. *Journal of Applied Polymer Science*, 118, 188–199. DOI: 10.1002/app.31986
441 Xu, Y. X., Kimb, K. M., Hanna, M. A., and Nag, D. (2005). Chitosan starch composite
442 film: preparation and characterization. *Industrial Crops and Products*, 21(2), 185-192.
443 DOI: 10.1016/j.indcrop.2004.03.002
444 Yan, Q., Hou, H., Guo, P., Dong, H., 2012. Effects of extrusion and glycerol content on
445 properties of oxidized and acetylated corn starch-based films. *Carbohydrate Polymers*,
446 87 (1), 707–712. DOI:10.1016/j.carbpol.2011.08.048
447 Zhijiang, C., Yi, X., Haizheng, Y., Jia, J., Liu, Y. (2016).
448 Poly(hydroxybutyrate)/cellulose acetate blend nanofiber scaffolds: Preparation,
449 characterization and cytocompatibility. *Materials Science and Engineering C*, 58, 5760,
450 757-767. DOI:10.1016/j.msec.2015.09.048
451
452
453

454 **Table 1.** Values of a , b coefficients and R^2 in the relationship between WVP
 455 and mg (PCL, PLA or PHB) · cm⁻²

Coating layer	Model	a	b	R^2
PCL	exponential	-0.478	4.00E-17	0.992
PLA		-0.413	3.00E-17	0.928
without TPCS		-0.351	2.00E-17	0.983
PHB		-0.425	2.00E-17	0.936
without TPCS		-0.378	1.00E-17	0.947

456

457 **Table 2.** Values of a , b coefficients and R^2 in the relationship between O₂P
 458 and mg (PCL, PLA or PHB) · cm⁻²

Coating layer	Model	a	b	R^2
PCL	exponential	-0.478	4.00E-17	0.992
PLA		-0.413	3.00E-17	0.928
without TPCS		-0.351	2.00E-17	0.983
PHB		-0.425	2.00E-17	0.936
without TPCS		-0.378	1.00E-17	0.947

459

460 **Table 3.** Contact angle values of the neat thermoplastic corn starch-based films, the
 461 developed multilayer structures and the neat PHB, PLA and PCL films.

Coating layer	mg · cm ⁻²	θ (°)
		54.8 (3.5) ^a
PCL	0.8	82.2 (2.5) ^b
	3.2	81.9 (3.0) ^b
	7	78.5 (4.4) ^b
PLA	0.5	84.0 (3.8) ^b
	3.2	84.1 (2.6) ^b
	4.9	83.2 (3.6) ^b
PHB	1.5	81.6 (2.6) ^b
	3.2	84.2 (2.4) ^b
	13.6	86.5 (3.1) ^b
PHB		123 (3.5) ^(*)
PLA		86.9 (1.6) ^(**)
PCL		89.5 (1.9) ^(***)

462 ^(*)Zhijiang *et al.*, 2016 ^(**)Darie *et al.*, 2014 ^(***)Campos *et al.*, 2008

463 a-b: Different superscripts within the same column indicate significant differences among samples ($p < 0.05$).

464

465 **Figure captions**

466 **Figure 1.** Surface images of the neat TPCS film (A) and the developed multilayer films
467 prepared with PCL (B), PLA (C) or PHB (D).

468 **Figure 2.** Cross-section images of the neat TPCS and multilayer films prepared with
469 PCL at different deposition times (A) TPCS, (B) 20 min, (C) 40 min and (D) 90 min.

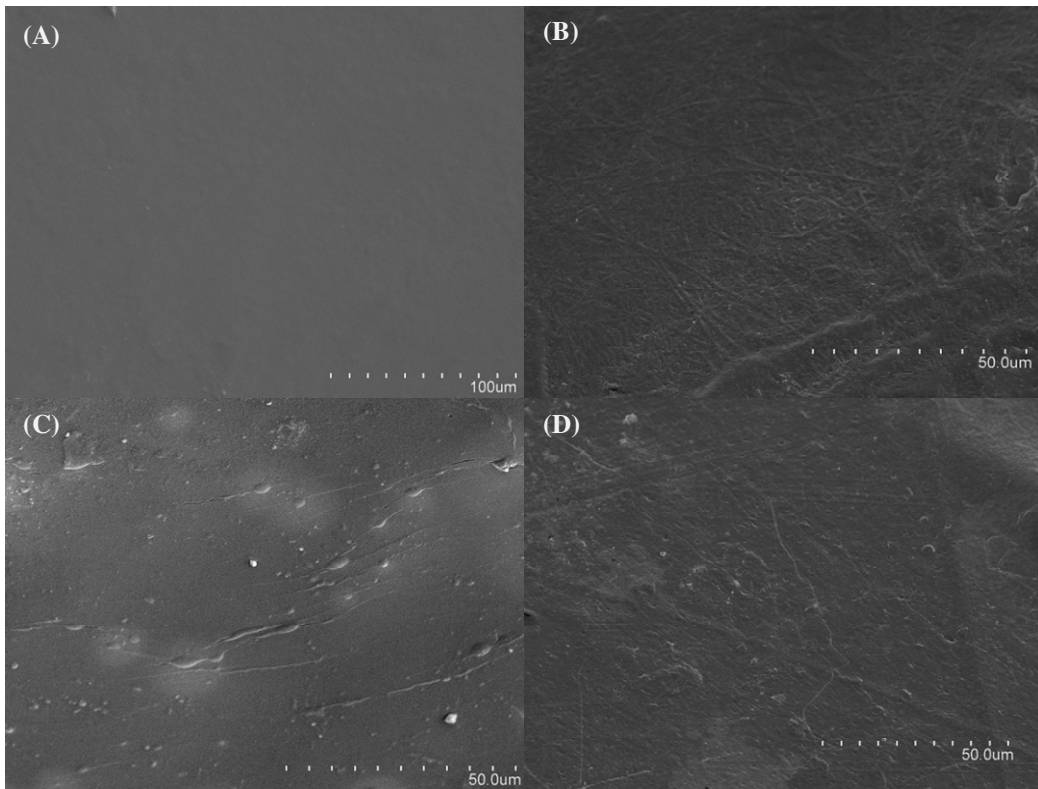
470 **Figure 3.** Cross-section images of the multilayer films prepared with PLA at different
471 deposition times (A) 2 min, (B) 20 min, (C) 40 min and (D) 60 min.

472 **Figure 4.** Cross-section images of the multilayer films prepared with PHB at different
473 deposition times (A) 20min, (B) 40 min, (C) 60 min and (D) 90 min.

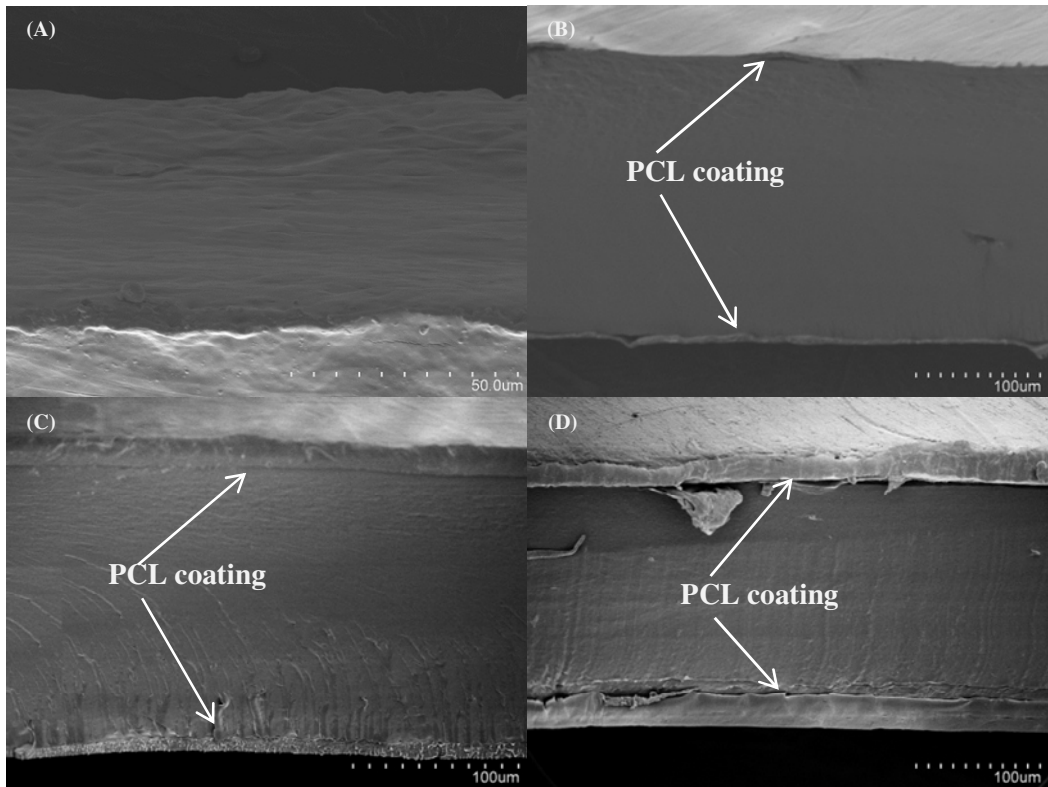
474 **Figure 5.** Relationships between WVP values *vs.* the mg electrospun coating \cdot cm²
475 (black symbols) and thickness *vs.* the mg electrospun coating \cdot cm² (white symbols).

476 **Figure 6.** Relationships between O₂P values *vs.* the mg electrospun coating \cdot cm² (black
477 symbols) and thickness *vs.* the mg electrospun coating \cdot cm² (white symbols).

478 **Figure 7.** Images of water droplet in contact angle measurements of the uncoated TPCS
479 film (A) and the developed multilayer films prepared with the highest deposited amount
480 of PCL (B), PLA (C) or PHB (D).



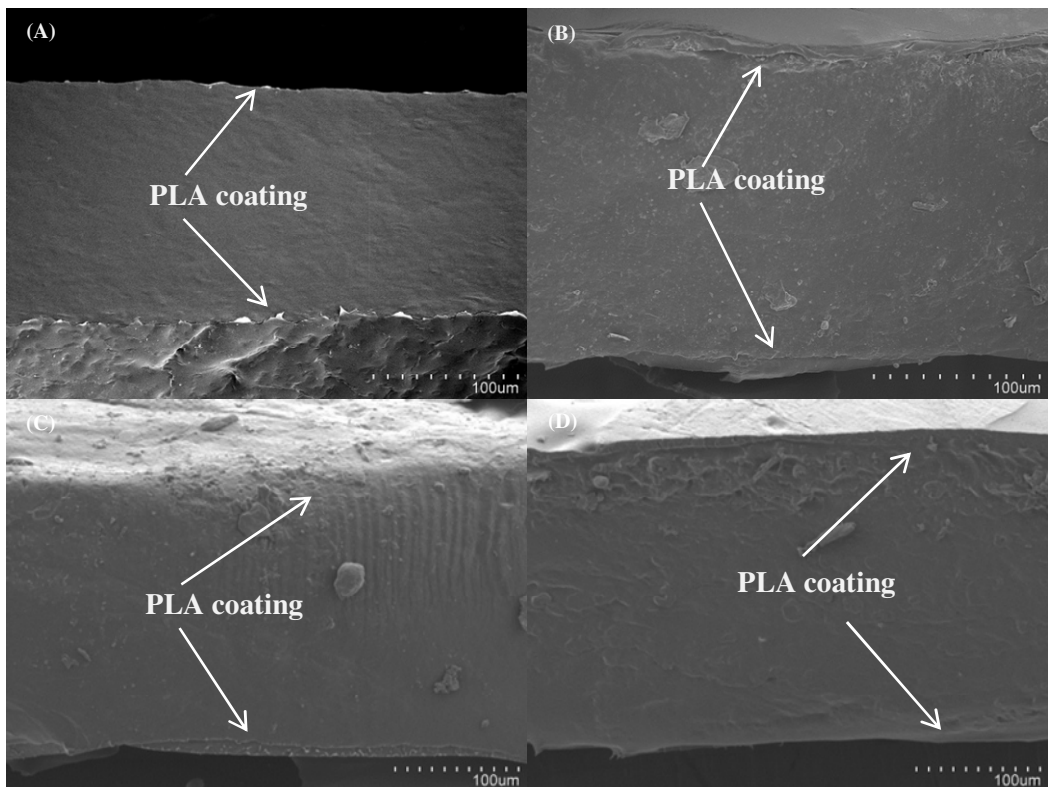
483 **Figure 2**



484

485

486 **Figure 3**

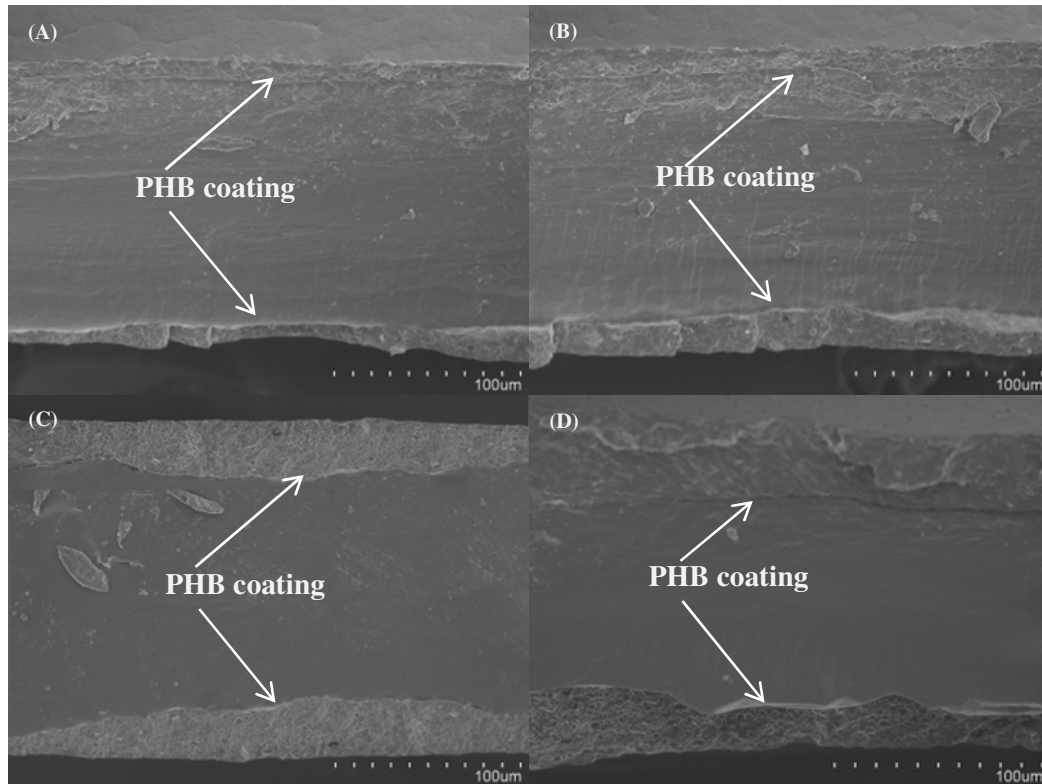


487

488

489

490 **Figure 4**



491

492

493

494

495

496

497

498

499

500

501

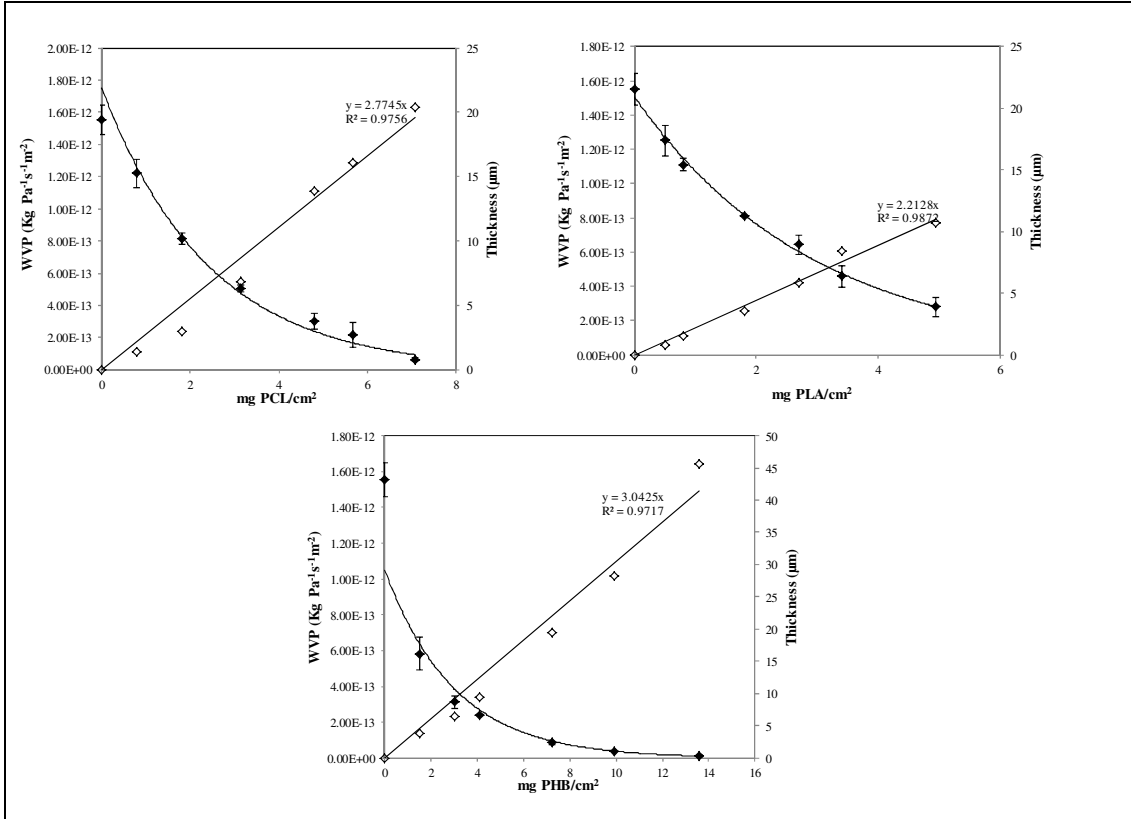
502

503

504

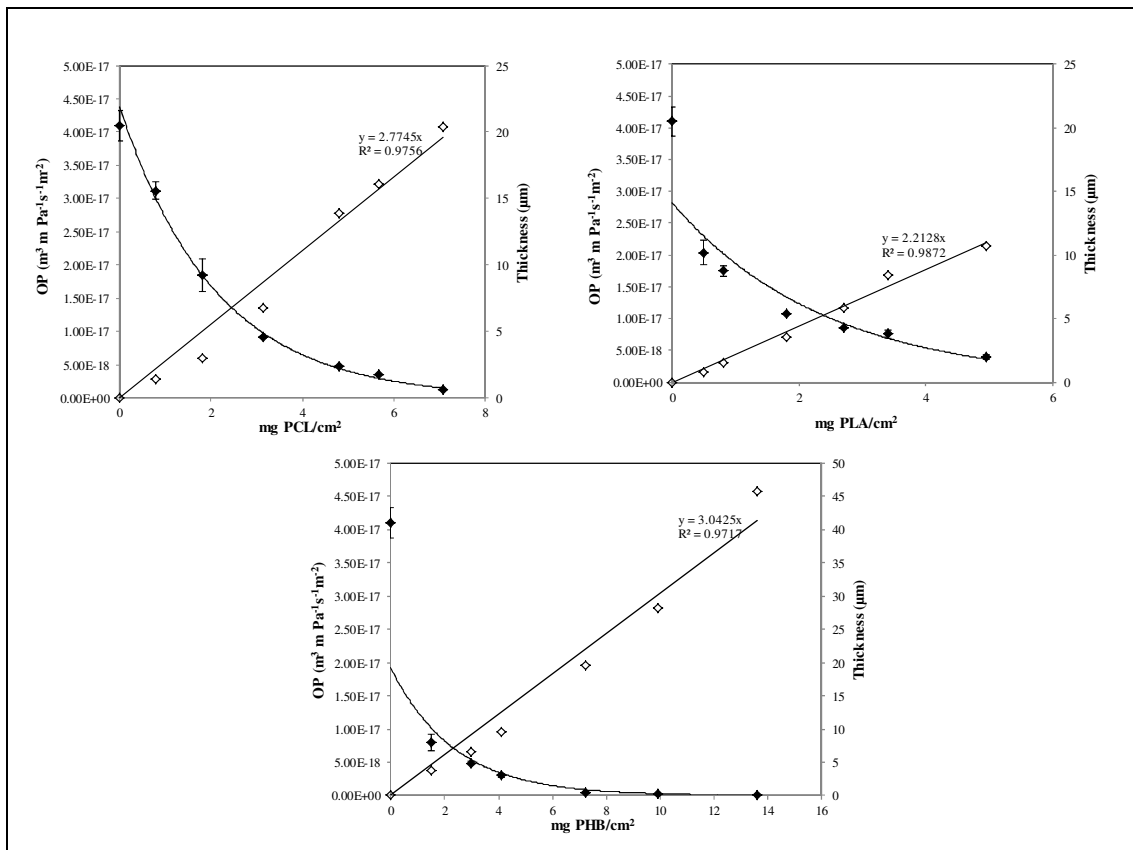
505

506 **Figure 5**



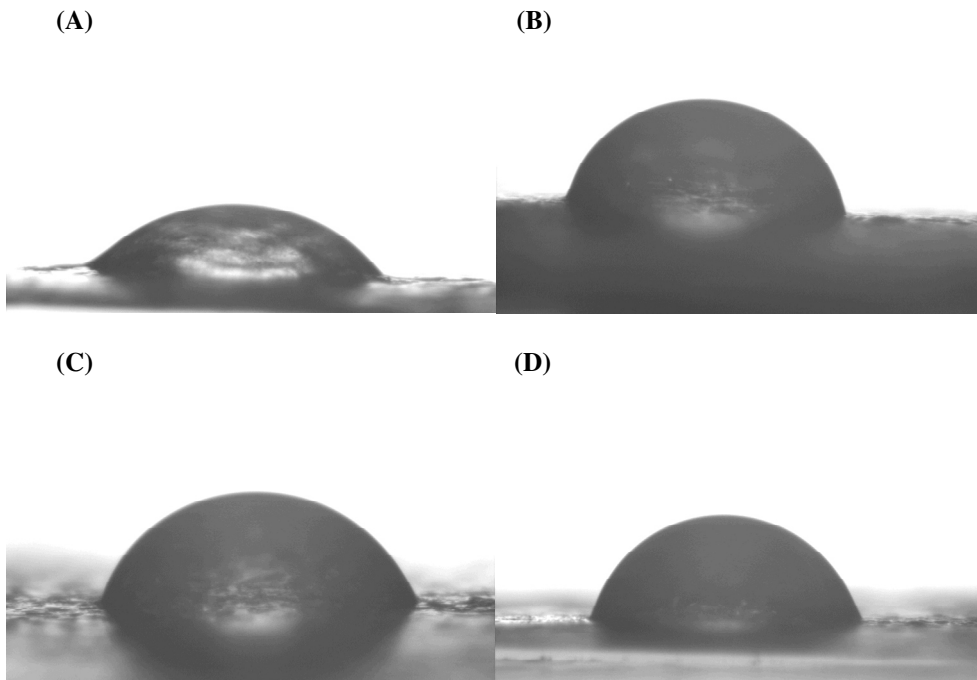
507

508



510

511



513

514